# Carbonate Preservation in Shallow Marine Environments: Unexpected Role of Tropical Siliciclastics

*Mairi M. R. Best,*[1] *Timothy C. W. Ku,*[2] *Susan M. Kidwell,*[3] *and Lynn M. Walter*[4]

*Earth and Planetary Sciences, McGill University, 3450 University Street, Montreal, Quebec H3A 2A7, Canada*
*(e-mail: mmrbest@eps.mcgill.ca)*

**ABSTRACT**

Coordinated taphonomic, geochronologic, and geochemical studies of bivalve death assemblages and their sedimentary environments of San Blas, Caribbean Panama, permit us to identify the major factors controlling skeletal degradation in mixed carbonate-siliciclastic tropical shelf sediments. Ten sites were studied along environmental gradients including water nutrients, grain size, and sediment chemistry (carbonate, organic carbon, and reactive iron contents). Taphonomic data were derived from naturally occurring bivalve death assemblages and experimentally deployed specimens of *Mytilus edulis* and *Mercenaria mercenaria* to determine environmental controls on types and intensities of postmortem damage to skeletal hardparts and to quantify short-term rates of damage accrual. Death assemblage shells were dated using $^{14}C$ and amino acid racemization techniques to examine shell persistence, scales of time averaging, and long-term rates of damage accrual, including correlations between shell damage and shell age. Pore water and sediment geochemical analyses were used to determine the pathways and extent of early diagenetic change in the different sediment–pore water environments. We found that carbonate shell preservation is enhanced in dominantly siliciclastic sediments compared to dominantly carbonate sediments. The most important factors limiting the postmortem persistence of shell material are (1) exposure above the sediment-water interface, which is enhanced in coarser-grained carbonate sediments and permits attack by bioeroders and encrusters; (2) the availability of abundant reactive iron mineral phases in the sediments, which promotes supersaturated pore waters and limits acid production; and (3) shell microstructure (rather than mineralogy), particularly organic content that is the focus of intense microbial attack. Thus, there is significant potential for enhanced carbonate shell preservation in areas receiving ferric-rich tropical weathering products, which are common in much of the tropics today and are associated with subduction systems in the geologic past. This suggests that paleodiversity estimates from carbonate tropical settings are minima and that siliciclastic settings are probably underestimated regions for carbon burial, given the large proportion of tropical shelf area characterized by such conditions and the relatively high proportional capture there of local carbonate production.

## Introduction

Carbonate skeletons provide the main record of the history of macrobenthic life (e.g., Behrensmeyer et al. 2000) and the main pathway for the transfer of carbon into the lithosphere (e.g., Berner 1983). The selectivities and rates of carbonate preservation are therefore of broad relevance to both the fossil record and the carbon cycle.

Maximum carbonate preservation has been thought to occur on tropical carbonate shelves due to high production rates and supersaturated waters (Opdyke and Walker 1992; Milliman 1993). Pore water chemistry of modern carbonate platforms, however, clearly shows that there is early and significant dissolution of carbonate within sediment pore waters (Morse et al. 1985; Walter and Burton 1990; Ku et al. 1999; James et al. 2005). In fact, dissolution of skeletal carbonates is a ubiquitous process in modern shelf environments; in carbon-

Manuscript received December 13, 2005; accepted October 13, 2006.

[1] Author for correspondence; present address: NEPTUNE Canada, University of Victoria, P.O. Box 1700 STN CSC, Victoria, British Columbia V8W 2Y2, Canada; e-mail: mmrbest@uvic.ca.

[2] Department of Earth and Environmental Sciences, Wesleyan University, 265 Church Street, Middletown, Connecticut 06459, U.S.A.

[3] Department of the Geophysical Sciences, University of Chicago, 5734 South Ellis Avenue, Chicago, Illinois 60637, U.S.A.

[4] Department of Geological Sciences, University of Michigan, 425 East University Avenue, Ann Arbor, Michigan 48109, U.S.A.

[The Journal of Geology, 2007, volume 115, p. 437–456]  0022-1376/2007/11504-0004$15.00

ate and noncarbonate shelves, an estimated 50% and 75%, respectively, of all produced carbonate is dissolved (Milliman 1993; Milliman and Droxler 1995). Siliciclastic shelves are generally expected to have negligible carbonate preservation (1) due to low carbonate production rates of heterotrophic organisms (Lees 1975; James 1997) and (2) based on studies in temperate settings, highly seasonal dissolution rates in undersaturated overlying waters, and/or pore waters (Alexandersson 1979; Aller 1982; Green and Aller 1998, 2001; but see Aller et al. 1996). Siliciclastics are thus considered to be of only minor importance in global carbonate burial budgets (e.g., Milliman 1993) and tend to be viewed with suspicion as sources of paleobiological information (e.g., Green et al. 1993).

Mixed carbonate-siliciclastic shelves have received increased attention from geologists (e.g., Mount 1984; Roberts 1987; Doyle and Roberts 1988; Alongi et al. 1996; Leinfelder 1997). However, very little information is available on carbonate preservation in siliciclastics from tropical settings, despite approximately one-half of all tropical shelf areas being of siliciclastic or mixed carbonate-siliciclastic composition (Best 1998). These settings are characterized by less seasonality and overall higher temperatures, which are expected to lead, on average, to increased carbonate and organic carbon production rates, more bioturbation (advection and sediment reworking), higher organic matter decomposition rates, and thus, probably higher carbonate dissolution rates, perhaps more than compensating for the higher production. Given the large number of physically and geochemically significant factors for carbonate preservation in tropical siliciclastic shelves and the range of positive and negative interactions they might have, we investigated whether net preservation of biogenic carbonate on such shelves is higher than, lower than, or little different from either temperate siliciclastic patterns or those of pure tropical carbonate shelves.

In 1994, we started a project examining skeletal carbonate preservation on the Caribbean continental shelf of Panama, where both carbonate and siliciclastic sediments are actively accumulating. Early results from both the Bocas del Toro region (Best and Kidwell 2000*a*, 2000*b*) and the San Blas Archipelago (Best 1996, 2000; Kidwell et al. 2001) indicated that, contrary to expectations, there was significant skeletal carbonate present in the siliciclastic sediments and that its state of preservation (taphonomic condition) was on par with if not better than that from carbonate sediments.

Those results led to this integrated taphonomic, geochronologic, and geochemical analysis of carbonate burial in tropical siliciclastics (Best et al. 1999*a*, 1999*b*, 2001; Ku et al. 2000). Bivalve mollusks became the taxonomic focus because they are common across environments, possess both calcitic and aragonitic shell layers, and have skeletal microstructures ranging from low to high organic content. From the range of tests summarized here, we find that, contrary to geological intuition, a variety of physical and geochemical factors promote preferential preservation of bivalve carbonate in tropical siliciclastics relative to carbonate sediments. This finding is of global significance given (1) the areal extent of shelves such as San Blas that receive siliciclastic debris from intense humid weathering of mafic island arc terrains and (2) the implications for the quality of the fossil record in such settings and for the burial of biogenic carbonate.

## Methods

***Study Area and Field Sampling.*** The San Blas Archipelago is located on the Caribbean coast of the Isthmus of Panama, between the Panama Canal and the Colombian border. The outer chain of coast-parallel cays is located approximately 20 km from the mainland. It is the surface expression of a semicontinuous barrier that extends east from Punta San Blas for more than 60 km and is associated with a broad range of carbonate sedimentary environments. Onshore, a series of short rivers, most having a small delta, deliver siliciclastic sediment derived from the humid tropical weathering of the San Blas Massif (fig. 1). The total drainage area is ~1500 $km^2$, and it receives >2000 mm $yr^{-1}$ precipitation (Cubit et al. 1989; D'Croz et al. 1999). The watershed rises steeply to 700 m above the coast and is largely drained by short, steep-gradient rivers, typical of mountainous humid tropics (e.g., Milliman and Syvitski 1992). This contrasts with more extensively studied large tropical river deltas such as the Amazon (Brazil) or Fly (Papua New Guinea) that drain extensive plains.

The San Blas Massif comprises a Cretaceous ophiolite complex composed of basalt, pillow lava, agglomerate, gabbro, diabase intrusives, chert, and siliceous limestones (Case 1974; Case et al. 1984; Escalante 1990). The massif is part of the Choco oceanic block, which overthrusts the Caribbean Plate to the north and rides on the subducting Nazca Plate to the south (Escalante 1990; Maury et al. 1995; Coates and Obando 1996). These ophiolites were intruded by quartz diorite plutons in the Early Tertiary (Kesler et al. 1977; Case et al. 1984). The Rio Gatun Fault, a sinistral strike-slip

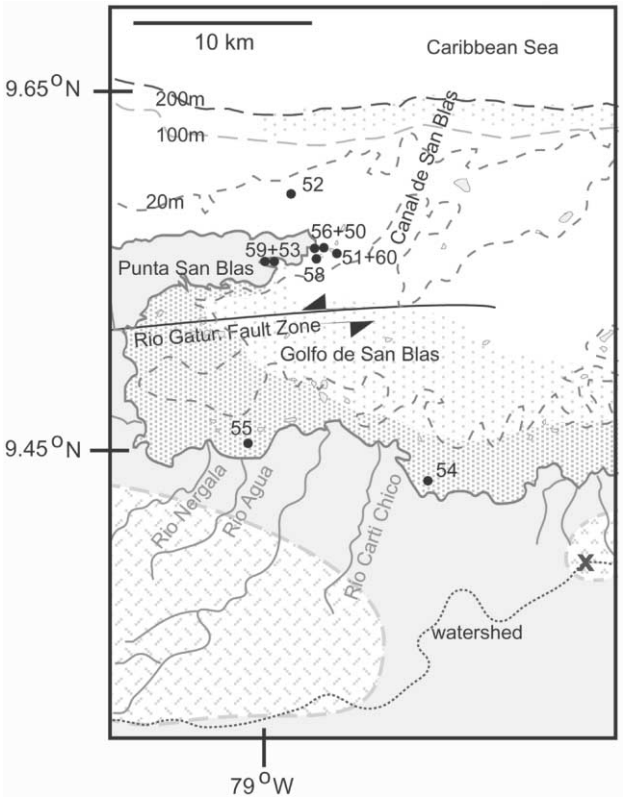


**Figure 1.** Map of the western San Blas area of Caribbean Panama. Numbered dots are locations of study sites with experimental shell arrays, samples of natural death assemblages, and pore water geochemical data. Sedimentary facies on the shelf include siliciclastic sediments (<30 wt% carbonate; *dark stipple*), mixed sediments (30–50 wt% carbonate; *light stipple*), and carbonate sediments (>50 wt% carbonate; *white*). Bathymetric contours (*dashed lines*) mark 20, 100, and 200 m. Topographic contour (*dotted line*) marks watershed; *X* is high-elevation point of 747 m. Mainland geology consists of a Cretaceous ophiolite sequence intruded by Early Tertiary quartz diorite (indicated by cross hatching). Map based on U.S. Department of Defense (1984) and Woodring (1957).

fault with vertical displacement toward the northwest, extends roughly east-west from the Canal Zone into the Golfo de San Blas (Woodring 1957; Kesler et al. 1990; Mann and Kolarsky 1995). Manganese enrichment in exhalative deposits occurs near Ensenada Mandinga, and Fe and Cu porphyry deposits related to intrusions occur at the far eastern end of the archipelago (Kesler et al. 1990).

Sediment plumes from rivers interact with a trade wind–driven coast-parallel current that runs between the outer and inner shelf cays and through the Canal de San Blas (D'Croz et al. 1999). Prevailing northeast trade winds shift to the north and northwest during the middle of the rainy season (September–November) when the Intertropical Convergence Zone moves northward to lie approximately at the same latitude as San Blas. The rainy season (May–December) is characterized by a rise in sea surface temperatures (January–April, 25.9°–26.7°C; May–December, 27.3°–28.2°C) and a drop in atmospheric pressure (January–April, 10.7–11.2 hPa; May–December, 9.7–10.6 hPa; Sadler et al. 1987). The tidal range is microtidal (<0.5 m; D'Croz and Robertson 1997).

Known as the Comarca de San Blas or Kuna Yala, the San Blas coastal archipelago is the autonomous home of the Kuna Indians, whose low-impact lifestyle, veneration of the mainland, and strict control of access to the area result in a region with limited anthropogenic effects (lack of forestry and mining, limited fisheries depletion, and subsistence agriculture; see Clifton et al. 1997). The Smithsonian Tropical Research Institute San Blas Marine Station, which served as a fieldwork base, was located on one of the cays off Punta San Blas at the western end of the region (it has since been closed; Alper 1998). Through this field station, the area was the site of many studies for more than 20 yr (Shulman and Robertson 1996; Clifton 1997; Clifton et al. 1997; D'Croz et al. 1999). These largely focused on the marine biology of the reefs off Punta San Blas and adjacent cays. Exceptions were the work by Freile (Freile and Hillis 1997) on *Halimeda* sediment production near Pico Feo and by Sare (Sare and Humphrey 1997) and MacIntyre (MacIntyre et al. 2001) on the geology and hydrogeology of the outer carbonate cays.

Shelf seawaters, subtidal sediments, and pore waters were sampled using a variety of shipboard and scuba techniques, including box and cylinder cores and grab samples (for details, see Best 2000 and forthcoming; Ku 2001; Ku and Walter 2003). Subtidal sedimentary environments of the San Blas shelf are divided into siliciclastic (<30 wt% carbonate), carbonate (>50 wt% carbonate), and mixed (30–50 wt% carbonate) facies, based on the weight percent bulk carbonate content as described in "Pore Water and Sediment Chemistry" (fig. 1, table 1). Pore water chemistry was studied at the nonreefal sites within the study area (as defined in table 1). Sedimentation rates are not explicitly known for these sites but are estimated from sediment accumulation on experimental arrays deployed for 3 yr. The $^{210}$Pb results indicate siliciclastic sedimentation rates on the order of 0.5–2.5 cm yr$^{-1}$ in siliciclastic sites, which is consistent with that observed with the experimental arrays (M. M. R. Best,

**Table 1.** Environmental and Sedimentary Data for Sites

| | | | Bottom water | | | Sediment | | | | | | |
|---|---|---|---|---|---|---|---|---|---|---|---|---|
| Composition, site name | Site no. | Environment | Depth (m) | Nutrients | Turbidity | Surface | Cover | Grain size | Fe-HCl (wt%) | Bulk $CaCO_3$ (wt%) | Mud $CaCO_3$ (wt%) | Mud organic carbon (wt%) |
| Siliclastic: | | | | | | | | | | | | |
| Rio Agua | 55 | River delta on mainland coast | 10 | Mesotrophic | Moderate-high | Soupy-firm | Sparse *Halophila* | Muddy sand | 4.87 | 29 | 10 | 1.5 |
| Soledad | 54 | Nonriverine segment of mainland coast | 10 | Mesotrophic | Moderate-high | Soupy | Red bacterial films | Sandy clayey mud | 2.49 | 22 | 24 | 2.5 |
| Mixed: | | | | | | | | | | | | |
| Ulagsukun channel | 53 | Narrow mangrove-fringed inlet | 10 | Mesotrophic | Moderate-high | Soupy | None | Mud | 1.58 | 47 | 27 | 3.4 |
| Ulagsukun bench | 59 | Narrow mangrove-fringed inlet | 5 | Mesotrophic | Moderate-high | Soupy-firm | *Thalassia* and/or *Halimeda* | Muddy sand | 1.12 | 47 | 7 | 2.5 |
| Nonreefal carbonate: | | | | | | | | | | | | |
| Guigalatupo | 58 | Restricted lagoon in a carbonate cay | 3 | Oligo-mesotrophic | Low-moderate | Soupy | None | Mud | .06 | 89 | 76 | 4.2 |
| Pico Feo Lagoon | 50 | Floor of broad back-reef lagoon | 10 | Oligo-mesotrophic | Low-moderate | Firm | Sparse *Halophila*, *Halimeda*, and filamentous algae | Fine sandy silt | .17 | 91 | 84 | 1.4 |
| Pico Feo Seagrass | 56 | Sea grass flat within the same large lagoon | 5 | Oligo-mesotrophic | Low-moderate | Firm | Dense *Thalassia* and *Halimeda* | Muddy sand | .19 | 92 | 80 | .8 |
| Reefal carbonate: | | | | | | | | | | | | |
| Korbiski reef wall | 51 | Leeward reef wall | 10 | Oligo-mesotrophic | Low | Firm | None | Coarse sand | NA | 99 | 74 | 1.4 |
| Korbiski reef flat | 60 | Edge of leeward reef flat | 5 | Oligo-mesotrophic | Low | Firm | None | Coarse sand | NA | 99 | 63 | 1.1 |
| Barrier channel | 52 | Channel through a windward reef crest | 10 | Oligotrophic | Low | Firm | None | Very coarse sand | NA | 100 | 95 | .0 |

Note. In addition to bulk analyses, separate analysis of the mud fraction has been used to clarify the nature of the matrix (mud) versus the coarse fraction. Sediment data are averages of grab samples and shallow cores (upper 20 cm); Fe-HCl is the sediment iron extracted by the boiling-HCl extraction method of Berner (1970). Water characterization is based on quantitative measurements (phosphate, nitrate/nitrite, silicate, visibility) summarized from Best (2000). NA = not applicable.

unpublished data). Generally, coastal siliciclastic sedimentation rates tend to be similar to, if not an order of magnitude greater than, carbonate sedimentation rates (Kukal 1990).

***Shell Material for Taphonomic Analysis.*** Taphonomic analysis focused on 10 sites at depths of 3–10 m, across a range of sediment composition (22–100 wt% carbonate, 0.8–4.2 wt% organic carbon, 0.06–4.87 wt% iron), grain size (coarse sand to clayey mud), water chemistry (oligotrophic to mesotrophic), and biological community (reef, sea grass, soft-bottom benthic; table 1, summarized from quantitative data in Best 2000). Skeletal death assemblages were collected at the 10 sites by washing a minimum of three replicate 5-L grab samples through 8-mm and 2-mm sieves, with the taphonomic study focusing on the coarser fraction. In addition, two commercially available temperate-latitude species of bivalves, *Mercenaria mercenaria* and *Mytilus edulis*, were experimentally deployed to test the effect of exposure above, at, and 20 cm below the sediment-water interface over periods of 9–27 mo. These two species provide contrast in shell microstructure, mineralogy, and robustness (*M. mercenaria*, thick, low-organic aragonitic shell; *M. edulis*, thin, high-organic aragonite + calcite shell; Taylor et al. 1969, 1973). Unless otherwise specified, results are for all deployment periods.

***Macroscopic Multivariate Taphonomic Analysis.*** To characterize their state of preservation, bivalve shells from both natural death assemblages (~200 specimens >8 mm per site) and experimental arrays (8 valves/taxa/treatment/array) were examined under ×10 magnification using a stereographic microscope and coded for variables describing encrustation, bioerosion, margin modification, fragmentation, fine-scale surface alteration (by microstructural sector), and color alteration. Fine-scale surface alteration ranges from loss of original luster to a fine-grained roughening or spalling of the surface and may be the product of microboring, maceration, abrasion, and/or corrosion, which are distinguishable only via scanning electron microscope (SEM; texturally similar to "corrasion" of Brett and Baird [1986]). Observations were made on shell interiors because such damage would be largely postmortem, therefore damage estimates are a minimum. Macroscopic features were then further investigated on uncoated specimens in a JEOL-JSM 5800 LV SEM under low vacuum (magnifications up to ×5000). Compositional spectra of mineral precipitates were simultaneously produced using the Oxford Instruments ISIS-300 microanalysis beam.

Macroscopic taphonomic data are summarized as the percentage of shells from each sample that display a given variable (with a 95% confidence interval). A multivariate percentage frequency data set (31 variables) was further investigated using two-dimensional nonmetric (monotonic) multidimensional scaling (NMDS; in Systat 5.2.1) sample and variable ordinations, using Euclidean distance matrices in order to preserve common absences (other similarity measures commonly used with diversity data deemphasize or dismiss common absences, whereas these absences are significant with taphonomic data). The deployment positions, periods, and experimental taxa at each site were treated as distinct samples. Because the scaling and orientation are arbitrary in the solutions of NMDS, the axes can be rotated or reversed without misrepresenting the result, as only the relative distances among sites must be conserved. Groups within Euclidean matrices (bases of NMDS ordinations described above) were tested using ANOSIM (PAST ver. 1.37; Hammer et al. 2001). Separate matrices were compared using Mantel tests (Manly 1994; Sokal and Rohlf 1995), initially programmed in Visual Basic for Excel and confirmed in GenAlEx (Peakall and Smouse 2006).

***SEM Characterization of Nacre Tablet Degradation.*** To further track postmortem modification of shells at the microstructural level, we focused on the inner nacreous shell layer of *Mytilus* because it was expected to have high reactivity based on lab experiments (Glover and Kidwell 1993; Harper 2000). Nacre is a high-organic aragonitic microstructure composed of thin roughly hexagonal tablets (1–2 × 5–10 $\mu$m), each surrounded by a proteinaceous organic matrix (Taylor et al. 1969). Under SEM, nacre was characterized in terms of the degree and style of tablet degradation, including edge modification, holes, and loss of tablet definition (table 2).

***Shell Ages in Death Assemblages.*** Age control was based on analyses of single shell fragments by accelerator mass spectrometry (AMS; University of Arizona) of $^{14}C$, combined with amino acid racemization (AAR; Northern Arizona University), together yielding 45 dated shells (Kidwell et al. 2005). For AAR analysis, we used the procedure of Kaufman and Manley (1998), which yields precise separations of D and L enantiomers of aspartic acid and glutamic acid (Glu) from small shell fragments. To avoid variability in racemization rates within shells (Carroll et al. 2003) and among taxa, all specimens were sampled from a homologous position (posterior half used for AAR, umbo and anterior for AMS), and most dates are from a single bivalve genus (*Pitar*; 10 of 12 shells used to calibrate the age equa-

**Table 2.** Microstructural Modification of Nacre Tablets on the Interior Surface of *Mytilus edulis*, Observed Using Environmental Scanning Electron Microscopy at a Magnification of ×5000

| Shell source | Environment | Loose crystals | Margins | Holes | Tablet obliteration | Carbonate precipitates |
|---|---|---|---|---|---|---|
| Fresh shell | (Gold coated) | None | Sutured | None | None | None |
| Archived shell | (Lab) | All on top layer | Some sutured, mostly smooth | Small | None | None |
| Rio Agua | Siliciclastic sandy mud | 1–2 layers loose crystals visible | Smooth | Rare, elongate | None | Welding of tablets + authigenic minerals |
| Soledad | Siliciclastic clayey mud | Few on surface | Sutured, smooth, and scalloped | Few small, rare elongate | A couple of fragments on surface | Authigenic minerals |
| Ulagsuken channel | Mixed organic, rich mud | All, multiple layers | Lacy to star when tablet is discernible | Difficult to discern discrete holes | Almost complete | Secondary fine-grained texture |
| Ulagsuken bench | Mixed organic, rich muddy gravel | All, multiple layers | Lacy to comb when tablet is discernible | Abundant, small, and elongate | Pervasive | Not discernible |
| Guigalatupo | Carbonate mud | All, multiple layers | Comb, when tablet is discernible | Elongate | Pervasive | None |
| Pico Feo Lagoon | Carbonate sand | All, multiple layers | Lacy, when tablet is discernible | Elongate | Pervasive | None |
| Pico Feo Seagrass | Carbonate muddy sand | All, multiple layers | Lacy, star, and rounded, when tablet is discernible | Elongate and small | Pervasive | None |

Note. Shells analyzed here were deployed at experimental sites for 1 yr, buried 20 cm below the sediment-water interface. Characterization is based on >3 shells/treatment and >3 locations per shell. Edges of the tablets were categorized as sutured (tablet contacts not visible, i.e., organic matrix intact), smooth (initial loss of organic matrix), scalloped (tablet edges corroded, possibly from microbially produced $CO_2$), lacy, and comb or star structure (more advanced dissolution damage). Holes in the surface of the tablets were subdivided into small (<0.5 $\mu$m) or elongate. Tablets also displayed a loss of definition of the tablet form, which probably reflects advanced dissolution from undersaturated waters. Secondary precipitation of calcium carbonate produces a fine-grained, smooth-margined texture (as opposed to the concave margins above), a welding of tablet contacts, or distinct crystals of authigenic minerals.

tion, and 26 of 33 additional shells were dated by applying that equation to Glu AAR values; see Kidwell et al. 2005 for details). Because our aim was to determine maximum scales of time averaging per assemblage, we preferentially dated the poorest-condition shells at each site.

To test shell preservation state as a function of shell age, before dating, all shells were scored for macroscopic damage following the procedure described above for macroscopic multivariate taphonomic analysis. The first dimension of a two-dimensional NMDS ordination captured most of the variability, with pristine shells and highly damaged shells plotting at the opposite ends of the axis, so this was used as a proxy for damage (for two-dimensional plot, see Kidwell et al. 2005).

***Pore Water and Sediment Chemistry.*** Detailed analytical methodologies are given by Ku et al. (1999); Ku (2001); Ku and Walter (2003); and T. C. W. Ku, L. M. Walter, and M. M. R. Best, unpublished manuscript. Sediment and pore water samples were collected in diver-collected box cores (upper 24 cm) and push cores (upper ~80 cm) and processed in 2-cm (box cores) or 8–12-cm (push cores) intervals under an $N_2$ atmosphere. Pore waters for the nonreefal carbonate, mixed, and siliciclastic sites were extracted by centrifugation, filtered, and preserved for various measurements. Sediment and seawater pH's and temperatures were determined on-site. Total alkalinity was measured by the Gran titration method with a precision of $\pm 0.5\%$ (Gieskes and Rogers 1973). Pore water $\Sigma H_2S$ analyses were done with headspace gas chromatography. Anion ($SO_4^{-2}$, $Cl^-$) concentration was determined by ion chromatography and electrometric endpoint titration with $2\sigma$ precisions of $\pm 1\%$ and $\pm 0.2\%$, respectively. Concentrations of dissolved Ca were measured by inductively coupled plasma atomic emission spectrometry (ICP-AES) with precision of $\pm 1\%$ ($2\sigma$). The millimoles of excess $Ca^{+2}$ and $SO_4^{-2}$ reduced were calculated by comparing pore water $Ca^{+2}/Cl^-$ and $SO_4^{-2}/Cl^-$ values to those of the overlying seawaters.

Sediment samples were oven dried and homogenized for subsequent measurements. All sediment analyses were reported on a dry weight basis. Carbonate carbon and organic carbon analyses were done on both bulk sample and mud fractions using a Carbo-Erba NA-1500 elemental analyzer and the methods of Verardo et al. (1990; analyses done at Northern Illinois University by P. Loubere and E. Castenson). Sediment iron extractions were carried out using the boiling-HCl method of Berner (1970), and extractant Fe concentrations were measured by ICP-AES using gravimetric standards of similar matrices. Acid-volatile sulfur (mostly iron monosulfides) and chromium-reducible sulfur (CRS; elemental sulfur and pyrite) were measured using a modified extraction scheme of Canfield et al. (1986). Concentrations of CRS were considered to represent pyrite sulfur. Degree of pyritization (DOP) values quantify the degree to which the available iron has been converted into pyrite. The DOP is defined as the amount of pyrite iron divided by the amount of pyrite iron plus HCl-soluble iron (Berner 1970; Raiswell et al. 1994). In some sediments, the boiling-HCl method can overestimate the amount of iron available for pyritization (e.g., Raiswell and Canfield 1996), but this does not detract from the major conclusions of this article.

## Abundance and Nature of Carbonate

Samples from carbonate, mixed, and siliciclastic facies all contain significant skeletal carbonate. In particular, sediments where the dominant matrix is siliciclastic (mud, <30 wt% carbonate) contain up to 47 wt% bulk carbonate (table 1). This contrasts with temperate shelf siliciclastics such as those from Long Island Sound, an embayment that contains ~2 wt% $CaCO_3$ (e.g., Green and Aller 2001), and tropical siliciclastic shelf sediments of the Amazon (Aller et al. 1986) and Fly deltas (Alongi 1992), where little to no skeletal carbonate is reported (0.7–3.1 wt% $CaCO_3$). The production of skeletal carbonate in San Blas is not hindered by the high physical mobility of sediment such as seen in large river deltas (Aller et al 1986). Communities of macrobenthic carbonate-shelled organisms such as bivalves are thus able to become established in significant diversity and abundance.

In San Blas, siliciclastic facies contain predominantly molluscan bioclasts, which are abundant and probably benefit from the higher nutrient regime of the coastal waters. However, contrary to models of skeletal distribution (e.g., Lees 1975), skeletal material in these facies is not limited to heterotrophic organisms; *Halimeda* (carbonate green alga), which is a major source of carbonate production in tropical carbonates (e.g., Freile et al. 1995), is also present in a number of siliciclastic sites. Significant *Halimeda* input occurs on submerged river deltas (e.g., Rio Agua) and along the shallow margins of high-organic mixed carbonate-siliciclastic inlets (e.g., the Ulagsukun inlet). This is contrary to standard models of environmental association (Lees 1975; Mount 1984; Carannante et al. 1988), which suggest that *Halimeda* would not occur in turbid/high-nutrient areas associated with siliciclastic input. It is, however, consistent with

occurrences in the Balearic Islands of Spain (Fornos et al. 1992) and on the Mahakam delta of Indonesia (Granier et al. 1996; Roberts and Sydow 1997). In addition to bivalves and *Halimeda*, death assemblages from San Blas contain gastropods, echinoids, plant material (wood, leaves), and, where immediately adjacent to the small bioherms that form on highs of the submerged deltas and inlets, small amounts of coral and bryozoan fragments (for details, see Best 2000; Kidwell et al. 2001).

Bivalves and gastropods also dominate in nonreefal carbonate sites, with the exception of Pico Feo Seagrass, where *Halimeda* again plays an important role. In reefal sites, corals become a dominant source of skeletal material; they are also a significant source of bioclasts for areas of Pico Feo Lagoon immediately adjacent to patch reefs. Therefore, the main difference among sites in skeletal taxa, and therefore potential carbonate production rates, is between reefal sites and all nonreefal sites, regardless of sediment matrix composition.

## Evidence for the Differential Preservation of Carbonate

***Condition of Skeletal Carbonate—Death Assemblages.*** Bivalve death assemblages of the 10 experimental sites fall into three taphonomic groups based on the NMDS ordination of taphonomic data (ANOSIM, $P = 0.0108$): those from reefal carbonates, those from nonreefal carbonates, and those from siliciclastic and mixed facies. A significant correlation between this taphonomic ordination and that of sediment and water characteristics (Mantel test, $P = 0.030$) underlines the influence of environment on the taphonomic signature (fig. 2). Shells from reefal carbonates typically display extensive fine-scale surface alteration and high levels of bioerosion (exhibited by up to 90% and 70% of shells, respectively). Shells from nonreefal carbonates display a greater tendency for pervasive surface alteration (<40% on average show patchy alteration), some microboring (2%–20%), and lack of staining (≪15%). Shells from siliciclastic and mixed sediments display pervasive staining (40%–90%) and patchy surface alteration (>60% on average), which correlates with root etching and microboring.

***Condition of Skeletal Carbonate—Experimental Arrays.*** Shells deployed experimentally on posts and on string tethers for up to 27 mo indicate that, considering the entire study area and all treatments, the first-order control on shell persistence is exposure above the sediment-water interface (Best 2000). Exposure produces high levels of bioinfestation (encrustation and bioerosion) in both low-organic aragonitic *Mercenaria* and high-organic bimineralic *Mytilus* shells in all environments within the first year (fig. 3). Sediment texture, through its correlation with shell exposure above the sediment-water interface, is thus predicted to exert a strong influence on taphonomic state; shells from coarser-grained facies, which in this study area are dominantly reefal carbonate, should have higher frequencies of bioerosion and bioencrustation than shells from muddy facies, because of increased exposure. This prediction is borne out by patterns of damage in death assemblages, as described above.

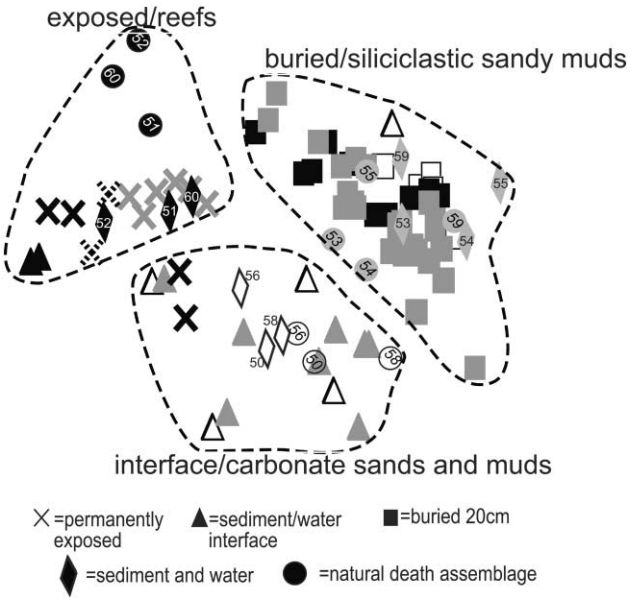


**Figure 2.** Overlain multivariate two-dimensional ordinations of taphonomic signature of bivalve death assemblage (stress 0.0553, *circles with site numbers*) and experimental shells (stress 0.1377, *x*'s, *triangles*, and *squares*), compared with an ordination of sediment + water analyses (stress 0.00548, *diamonds with site numbers*), using nonmetric multidimensional scaling. *Gray* = mixed and siliciclastic sites, *black* = reefal carbonates, and *outlines* = carbonate sands and muds. Rotated axes have been omitted for clarity; relative position of sites within ordinations has been preserved (see text).

For shells deployed at or below the sediment-water interface, shell condition is controlled primarily by early diagenetic reactions and thus a function of sediment composition. Shells buried at carbonate sites exhibit higher weight loss (*Mytilus*) and greater retreat of the margin of the inner shell layer from the commissure (*Mercenaria*) than shells deployed in siliciclastic sediments (Kruskal-Wallis,

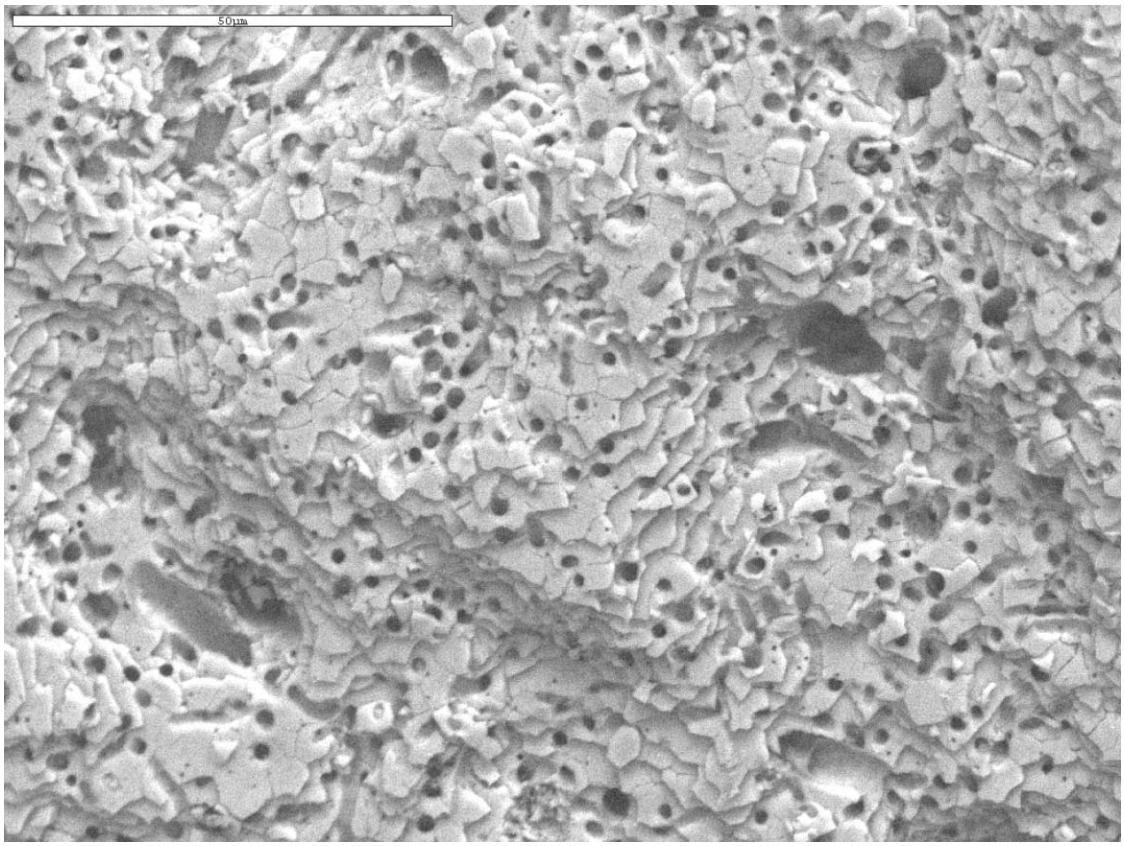


**Figure 3.** Microboring in nacre of a *Mytilus edulis* experimental shell exposed at the sediment-water interface in a reef environment for 1 yr, showing degree of shell degradation as a result of bioerosion. Scale bar is 50 $\mu$m.

$P < 0.05$), suggesting that carbonate sediments are less conducive to shell preservation. Weight loss is generally higher for shells deployed at the sediment-water interface than for continuously buried shells (Best 2000). This is presumably because the uppermost part of the sedimentary column is most likely to experience aerobic decomposition of organic input, resulting in corrosive pore waters (cf. Aller 1982).

The SEM examination of experimental shells highlights these differences and allows microstructural changes to be assessed (table 2; fig. 4). In carbonate sediments, both maceration of microstructural organic matrix and chemical dissolution of crystallites are evident (table 2; fig. 4*e*, 4*f*). By contrast, in the iron-rich siliciclastic sediments, shells are discolored due to precipitation of secondary minerals on shell surfaces, and shell modification is predominantly via microbial maceration of organic matrix; there is little or no evidence of pervasive chemical dissolution of first-order crystallites (fig. 4*c*, 4*d*). The energy dispersive spectroscopy analysis indicates that secondary precipitates on shells in siliciclastic sediments include iron-rich clays, iron carbonate, and calcium carbonate (Best 2000; Ku and Walter 2003).

Sequential observations over the 27-mo deployment indicate that weight loss and microstructural modification do not proceed linearly. Instead, modification occurs rapidly within the first year and then decreases as shells (1) are covered with epibionts during exposure, (2) lose the labile or readily accessible portion of their organic matter, and/or (3) are annealed with secondary mineral films (Best 2000).

***Shell Ages and Damage Levels in Death Assemblages.*** Based on 45 dated shells on the modern San Blas shelf (inside cays), surficial sediments are dominated by recently produced dead shells (fig. 5). However, death assemblages in siliciclastic sands and muds contain shells up to ~5400 yr old, with a median shell age of 375 yr, whereas median shell age in carbonate sediments is much shorter (72 yr), despite the inclusion in reef pockets of outlier 1–3-ka shells (Kidwell et al. 2005). These differences in apparent shell persistence are consistent with

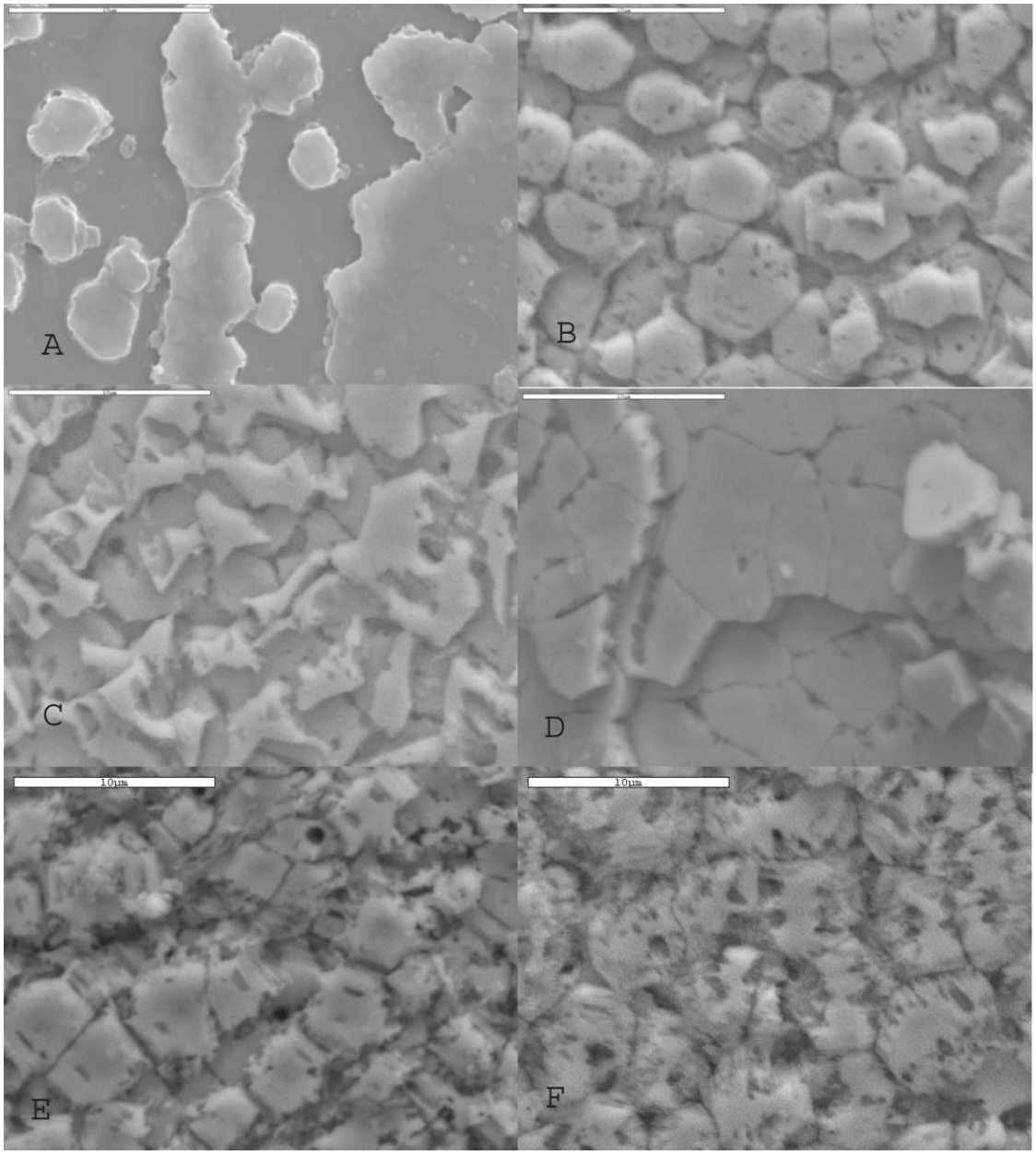


**Figure 4.** Environmental scanning electron microscopy images of damage levels to the inner nacreous layer of *Mytilus edulis* deployed experimentally in various sediment types for at least 1 yr, 20 cm below the sediment-water interface; magnification ×5000. *A*, fresh shell before deployment; *B*, shell exposed to atmosphere in laboratory for 1 yr (control); *C*, siliciclastic sandy mud (Rio Agua); *D*, siliciclastic clayey mud (Soledad); *E*, carbonate sand (Pico Feo); *F*, carbonate mud (Guigalatupo). See table 2 for distribution of features among sites. Scale bars are 10 $\mu$m.

differences in damage levels in both death assemblages and experimentally deployed shells (described above); bivalve shells from carbonate settings are in significantly worse condition from bioerosion, bioencrustation, and surface alteration at younger ages (fig. 5).

***Geochemical Evolution of Pore Waters and Sediments.*** Net calcium carbonate dissolution in pore waters can be recognized from excess $Ca^{+2}$ values, which compare pore water $Ca^{+2}/Cl^{-}$ ratios to the $Ca^{+2}/Cl^{-}$ ratios of the overlying seawater (e.g., Walter and Burton 1990; Ku et al. 1999). In San Blas sediments, excess $Ca^{+2}$ values ranged between −0.3 and +0.7 mM (fig. 6). Eighty-five percent of all pore

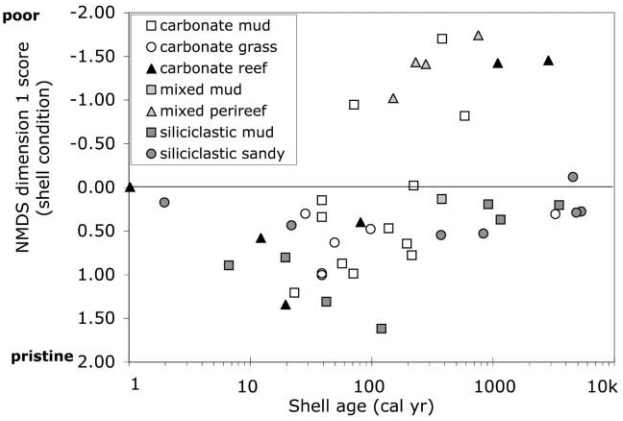


**Figure 5.** Relationship between shell age and shell condition, as scored by multivariate analysis (nonmetric multidimensional scaling [*NMDS*]) of taphonomic damage (adapted from Kidwell et al. 2005). Shells younger than ~100 yr in both siliciclastic and carbonate settings can exhibit a range of damage states, indicating that initial damage accrual is erratic but can be rapid in both settings. Based on the full age spectrum, however, shells from carbonates range up to poorer conditions than shells of similar or greater age from siliciclastic and mixed-composition sediments, suggesting more intense recycling in carbonate sediments. Maximum shell ages in the two sediment types differ significantly at $P < 0.02$ using extreme-value statistics (Kidwell et al. 2005). *cal yr* = calendar years.

waters had excess $Ca^{+2}$ values greater than 0, and in general, the highest excess $Ca^{+2}$ values were found in carbonate or mixed carbonate-siliciclastic sediments (fig. 6). Although excess $Ca^{+2}$ values ($\pm 0.2$ mM) of 0 were analytically indistinguishable from overlying seawaters, calculated aragonite saturation states decreased from +3.3 to +4.5 in overlying seawaters to near +1 (saturation) in the upper 2 cm of sediment (fig. 7). In all cases, aragonite saturation states then increased with sediment depth, indicating that chemical dissolution was dominantly occurring in the upper few centimeters of sediment (fig. 7).

Several chemical and isotopic pore water analyses (alkalinity, $SO_4^{-2}/Cl^-$, $Ca^{+2}/Cl^-$, $\delta^{34}S\text{-}SO_4$, $\delta^{18}O\text{-}SO_4$, $\delta^{13}C$–dissolved inorganic carbon, and potential sulfate reduction rates) indicated minor to modest degrees of organic matter oxidation, carbonate dissolution, and sulfate reduction across all sediment types (fig. 6; Ku 2001; T. C. W. Ku, L. M. Walter, and M. M. R. Best, unpublished manuscript). Elevated pore water $Fe^{+2}$ concentrations were observed in the upper 6 cm of the mixed composition and siliciclastic sediments, which indicated the presence of bacterial iron reduction (fig. 7). The mixed and siliciclastic sediments had high concentrations of total iron (1.2–6.9 wt%) and HCl-soluble iron (0.8–5.4 wt%; table 1 for averages; fig. 7; Ku 2001). These sediment iron concentrations are significantly higher than those found in nearshore temperate sediments, but they are similar to sediment iron concentrations found in tropical shelf sediments near the Amazon River and the Gulf of Papua (Aller et al. 1986; Alongi et al. 1993; Raiswell and Canfield 1998). In contrast, the carbonate sediments had much lower total iron (0.1–0.3 wt%) and HCl-soluble iron (0.04–0.22 wt%) concentrations (table 1 for averages; fig. 7; Ku 2001). For all sediments, pyrite sulfur concentrations ranged from 0.09 to 3.1 wt% and generally increased down core, resulting in higher DOP values at greater sediment depth (fig. 7; Ku 2001; T. C. W. Ku, L. M. Walter, and M. M. R. Best, unpublished manuscript). Excluding the three deepest intervals of the Rio Agua (site 55) core, the average DOP value of the carbonate sediments was 0.62, which was significantly higher than the average of the mixed and siliciclastic sediment value of 0.11 (fig. 7; Ku 2001). Thus, most of the iron in the carbonate sediments was converted into pyrite in the upper 20 cm, while on average, only 11% of iron in the mixed and sil-

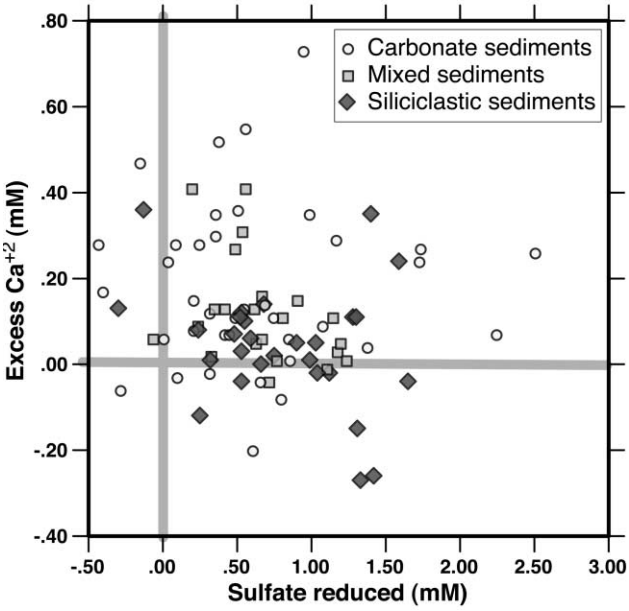


**Figure 6.** Excess calcium versus sulfate reduced in San Blas nonreefal sediment pore waters. Most of the pore waters had positive excess calcium values and modest degrees of sulfate reduction. The carbonate sediments generally had the highest excess calcium values.

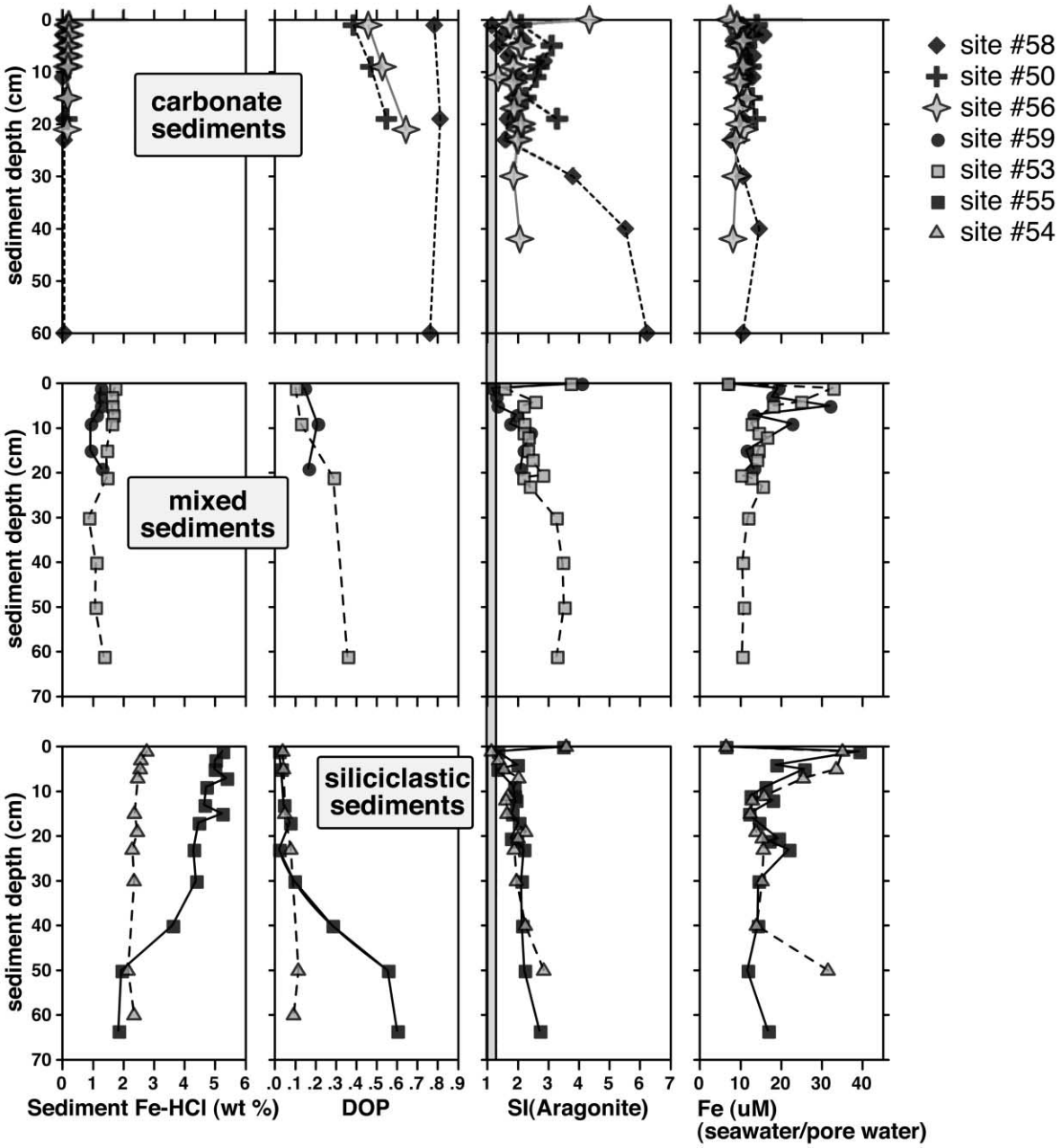


**Figure 7.** Sediment depth versus sediment and pore water chemistry for San Blas nonreefal carbonate, mixed, and siliciclastic sediments. Fe-HCl is the sediment iron extracted by the boiling-HCl extraction method of Berner (1970) and represents the concentration of available iron that could be converted into pyrite. Degree of pyritization (*DOP*) values represent the fraction of available sediment iron that has been converted into pyrite (see text). Overlying seawater and pore water aragonite saturation indexes (*SI*) were calculated using apparent seawater equilibrium constants for aragonite and the carbonic acid system after adjusting for temperature, salinity, and boric acid (Mehrbach et al. 1973; Millero 1979, 1995; Mucci 1983). Pore water Fe concentrations are also given, distinct from sediment iron concentrations. Seawater values are shown at zero sediment depth.

iciclastic sediments was sulfidized. Note that the DOP values at the restricted carbonate cay lagoon (site 58) were constant, with sediment depth at ~0.8 cm (fig. 7).

## Factors Controlling Differential Preservation

The broad range of environments available on the San Blas shelf allows us to investigate the effects of sediment composition (grain size, carbonate, organic carbon, iron) on the preservation of skeletal carbonate. Across both siliciclastic and carbonate environments, both death assemblages and experimental shells show that the dominant control on skeletal degradation is exposure to bioeroders at or above the sediment-water interface (e.g., fig. 3; Best 2000 and forthcoming). During burial, multiple lines of evidence (macroscopic appearance, weight loss, SEM of nacre, shell ages) indicate that shell preservation is favored in siliciclastic facies. Pore water analyses document that (1) chemical dissolution is more important in carbonate than siliciclastic settings, (2) it occurs primarily in the upper zones of the sediment, and (3) early diagenetic conditions are fundamentally different between siliciclastic and nonreefal carbonate sediments. In the following sections, we discuss how these patterns are a function of sediment composition.

***Exposure and Exhumation of Shells Promote Bioerosion.*** Based on both experimental arrays and observations on natural death assemblages, bioerosion and dissolution are the two most aggressive processes of carbonate shell destruction in the San Blas study area, and both can be linked to exposure and repeated burial-exhumation cycles at the sediment-water interface.

Our experimental arrays indicate that if a shell is not buried rapidly after death, it is subject to immediate bioerosion, and even shells that are only temporarily or intermittently exposed (e.g., those loosely tethered at the sediment-water interface) become infested (Best 2000). In death assemblages, frequencies of bioeroded shells are higher in carbonate sites that are also coarser grained (less mud), whereas the generally finer grain sizes encountered in mixed and siliciclastic sites tend to coat shells at the sediment-water interface, excluding infesters. In the muddiest siliciclastic sites, a significant nepheloid layer is common, and the sediment-water interface is generally soupier in consistency. These conditions should degrade living conditions for bioeroding and microboring animals by reducing available light and oxygen and reducing the efficiency of filter feeding (e.g., for boring sponges). In the absence of rapid burial, bioerosion destroys skeletons at rates that are orders of magnitude faster than chemical dissolution (e.g., Hutchings 1986).

The grain size and mass properties of sediment and local bioturbation intensity determine whether a shell is buried. Although we have no quantitative information, qualitative observations indicate that shell exhumation by advecting bioturbators is higher in carbonate sites and particularly the reefs. Specifically, coarser-grained (carbonate) sites are characterized by larger numbers of shells exposed at the sediment-water interface and by higher densities of active callianassid shrimp mounds, and net sediment increase was rarely observed against the posts of our experimental arrays, all in contrast to siliciclastic sites. We thus infer more frequent burial/exhumation cycles and assume greater seawater advection into the sediments. In general, particularly in the tropics, carbonate sediments tend to be coarser grained on average because of the in situ production of large grains. By contrast, siliciclastic sites not only are distal from the sediment source, with resultant sorting, but are also often sheltered behind a carbonate barrier (as seen in San Blas), which dissipates wave energy that might otherwise winnow muds from muddy sands of the coastal deltas. Sedimentation rates also affect shell burial rates. Again, the tendency is for carbonates to have lower net accumulation rates than siliciclastics (Kukal 1990), therefore increasing the likelihood of extended exposure in carbonate compared to siliciclastic facies.

Sediment mass properties and bioturbation intensity not only influence the exposure of shells to bioerosion but also control pore water mass transport and oxygen levels within the sedimentary column. These in turn are key ingredients for carbonate dissolution reactions during early burial, as discussed in the next section.

***Taphonomic and Geochemical Evolution within San Blas Sediments.*** In addition to differences in levels of damage from bioerosion, San Blas death assemblages and experimental shells both reveal differences in chemical dissolution between carbonate (sites 50, 56, 58), mixed composition (sites 53, 59), and siliciclastic facies (sites 54, 55). Shells in carbonate sediments display the most extensive dissolution features and also have lower median shell ages (table 2; figs. 4, 5).

As possible causes of this difference, consider the two most important organic matter oxidation pathways in coastal sediments affecting carbonate dissolution, namely, oxic respiration and sulfate reduction (Jorgensen 1982; Canfield and Raiswell

1991). During oxic respiration, pH decreases, and $SI_{aragonite}$ decreases to values <1 due to the addition of $H_2CO_3$ and the oxidation of ammonia to nitrate. During the initial stages of sulfate reduction, carbonate undersaturation and $SI_{aragonite}$ evolution depend on how completely $H_2S$ is removed from solution. If $H_2S$ is allowed to accumulate in solution, the $H_2S$ buffers the pH to values slightly below 7 and causes aragonite undersaturation; aragonite supersaturation occurs only after significant alkalinity is produced by sulfate reduction (e.g., Ben-Yaakov 1973). However, when abundant reactive sedimentary Fe is present, $H_2S$ readily precipitates from pore water, causing pH to rise; the saturation index for aragonite quickly reaches saturation and progresses to supersaturated conditions (Canfield and Raiswell 1991). If such sediments are remixed into the oxidized sediment layer, reduced $H_2S_{(aq)}$ or solid iron sulfide can be reoxidized, producing acid and relowering the saturation state of aragonite. Where it occurs, iron reduction also figures into aragonite saturation levels because of its production of alkalinity and suppression of the sulfate reduction zone within the sedimentary column (see discussion at the end of this section).

In San Blas, pore waters at carbonate back-reef lagoon sites (50, 56) show only minor evidence for sulfate reduction and carbonate dissolution, slightly elevated alkalinities compared with levels in overlying seawaters, and $SI_{aragonite}$ values greater than 1 (figs. 7, 8). Figure 8 shows the $SI_{aragonite}$ versus alkalinity values of the San Blas pore waters and the theoretical pore water evolution lines of oxic respiration, complete $H_2S$ precipitation, and no $H_2S$ precipitation following the closed system approach of Ben-Yaakov (1973) and Canfield and Raiswell (1991). The aragonite saturation states and the modest alkalinity concentrations of the back-reef lagoon sediments (50, 56) indicate that the observed carbonate dissolution likely occurred during oxic respiration or the early stages of sulfate reduction or by sulfate reduction–sulfide oxidation cycles (fig. 8; see scenario described in Walter and Burton 1990; Ku et al. 1999). The lack of more pronounced pore water evidence for carbonate dissolution is somewhat puzzling considering the death assemblage and experimental shell results, but the lack may be due to relatively low concentrations of organic carbon (0.8–1.4 wt% in the mud fraction) and/or to rapid pore water–seawater exchange associated with relatively large grain sizes (muddy sands to sandy silts). Mass transport processes were seemingly rapid enough to exchange out pore water that contained dissolved sulfide and/or to lower pH values below those expected during the early stage of sulfate reduction. Note that our pore water comparison does not include reef gravels, where this effect of grain size and exposure is even more extreme (Best 2000 and forthcoming). Other workers have noted that pore water concentrations may be poor indicators of the importance of early diagenetic reactions, especially in nearshore carbonate sediments that typically have high bioirrigation rates (e.g., Furukawa et al. 2000).

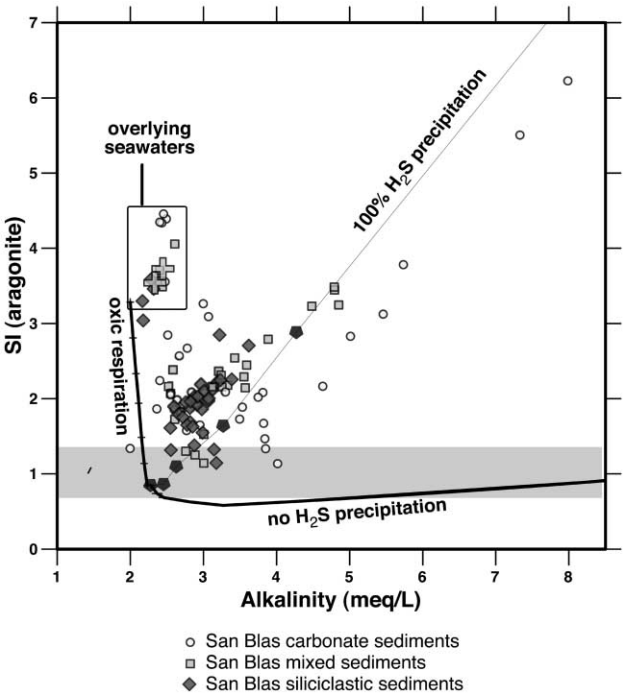


**Figure 8.** Closed system early diagenetic evolution of pore waters. The model begins with seawater at 1 atm, 25°C, and pH = 8.1. Standard surface seawater is supersaturated with respect to aragonite ($SI_{aragonite}$), and the following composition is assumed: $\Sigma CO_2 = 2.2$ mM, $PO_4^{-3} = 1$ $\mu$M, borate = 420 $\mu$M, $O_2 = 300$ $\mu$M, $NO_3^- = 16$ $\mu$M (Broecker and Peng 1982). Marine phytoplankton with Redfield C : N : P ratios is considered the organic carbon source, and aragonite saturation indices were calculated as explained in the figure 7 legend. The oxic respiration line shows the complete utilization of dissolved $O_2$, as explained in the text. Model lines representing the fate of produced sulfide from bacterially sulfate reduction are shown: "100% $H_2S$ precipitation" and "no $H_2S$ precipitation."

In addition to mass transport, another feature of the San Blas carbonates that may have obscured the pore water reactions is their noncarbonate content (89%–92% $CaCO_3$ in the bulk sediments and 76%–84% $CaCO_3$ in the mud fraction; table 1). The

ranges of Fe-HCl and pyrite sulfur in these carbonate sediments were 38–2600 ppm (1100–3700 ppm total Fe) and 1300–4300 ppm, respectively (table 1; Ku 2001; T. C. W. Ku, L. M. Walter, and M. M. R. Best, unpublished manuscript). This contrasts with "pure" bulk carbonate sediments from Florida Bay and the Bahamas, which have >98% $CaCO_3$ and 30–100 ppm total iron (Morse et al. 1985; Walter and Burton 1990). Although the iron concentrations in the San Blas carbonate sediments were low compared with the San Blas mixed and siliciclastic sediments, there may have been enough iron present to remove significant quantities of pore water $H_2S$. Pore water $H_2S$ concentrations in San Blas carbonate sites were below detection limits, and DOP values ranged between 0.39 and 0.81 (fig. 7). At Pico Feo (sites 50 and 56), the DOP values increase consistently with sediment depth to values between 0.55 and 0.64, indicating that not all of the reactive iron phases have been sulfidized (fig. 7). The HCl iron extraction may overestimate the amount of reactive iron resulting in low DOP values, but this is unlikely since the DOP values at carbonate site 58 were between 0.76 and 0.81 (fig. 7). It is more likely that all of the available iron has been sulfidized in the carbonate sediments of Guigalatupo (site 58, described in the next paragraph) and not in the carbonate Pico Feo sediments (sites 50 and 56). Thus, mineral sulfide oxidation via bioturbation and bioirrigation may be a significant carbonate dissolution process in these sediments.

Unlike the other San Blas carbonate sites, the Guigalatupo carbonate cay lagoon (site 58) sediments were covered with a significant nephaloid layer that produced skeletal degradation patterns due mostly to burial processes. Uniform death assemblage surface alteration patterns and distinctive comb structures in the nacre of experiment shells, without overprinting of extensive microboring, indicate that chemical dissolution was pervasive in these sediments (figs. 3, 4; Best 2000 and forthcoming). In addition, the death assemblages here displayed an anomalously high proportion of articulated shells (indicating input within a year, based on experiments reported in Best et al. 2004) and young shell ages compared with other carbonate sites (Kidwell et al. 2005). Pore waters at this site approach undersaturation at ~4 meq $L^{-1}$ alkalinity and then rise to much higher alkalinity and aragonite saturation states (fig. 8). As noted above, the sediment DOP values show that much of the reactive iron has been sulfidized; thus, dissolved sulfide could persist in the pore waters and lower carbonate saturation states. Most of the dissolution likely occurs in the upper 25 cm of sediment since $SI_{aragonite}$ values significantly increase at greater depths (fig. 7). These chemical observations are consistent with the taphonomic data above, all of which point to rapid shell loss by predominantly chemical processes at this site.

Pore waters from San Blas mixed (sites 53, 59) and siliciclastic (sites 54, 55) sediments were slightly supersaturated with respect to aragonite and had alkalinities between 2.4 and 4.9 meq/L (fig. 8). The $SI_{aragonite}$ values from these sites were lower than their overlying seawaters, with a minimum of ~3 meq/L alkalinity. Further increases in alkalinity follow the 100% $H_2S$ precipitation pathway, which results in higher $SI_{aragonite}$ values, indicating better conditions for carbonate preservation with continued organic matter decomposition (fig. 8). The lowest $SI_{aragonite}$ values occur in the upper few centimeters of these sediments and are most likely caused by oxic respiration. Reactive iron phases, as represented by Fe-HCl, would immediately precipitate any produced $H_2S$, thereby quickly raising the aragonite saturation state following the 100% $H_2S$ precipitation model line (fig. 8). The concentrations of pyritic sulfur and the DOP values in the upper few centimeters of the mixed and siliciclastic sediments indicate that sulfide is rapidly removed from pore water solutions (fig. 7; Ku and Walter 2003). DOP values increase with sediment depth, showing continued sulfidization of the sedimentary iron (fig. 7). The mixed and siliciclastic sediments contain abundant quantities of iron phases that remove any produced sulfide from these pore waters, thus favoring carbonate mineral supersaturation and promoting carbonate precipitation, not dissolution. This is consistent with SEM observations of secondary carbonate precipitates on experimentally deployed *Mytilus edulis* (Best 2000).

The high concentrations of HCl-soluble iron phases in siliciclastic-rich sediments may also promote carbonate preservation by limiting sulfate reduction and subsequent sulfide oxidation. In the mixed and siliciclastic sediments, 67%–91% of the Fe-HCl is ferric iron and a significant fraction of this ferric iron exists in clay minerals belonging to the verdine facies (Odin 1990; Ku and Walter 2003). Recent experimental studies have provided direct evidence that bacteria can couple silicate iron reduction with organic carbon oxidation (e.g., Kostka et al. 1996, 1999). In other tropical, iron-rich shelf sediments, it has been suggested that iron-reducing bacteria outcompete sulfate-reducing bacteria for organic matter, thereby suppressing sulfate reduction in zones of intense iron reduction (Aller et al. 1986; Alongi 1995). If this were occurring in San Blas, acid formation by reactions between sulfide

minerals and oxygenated seawater would be limited because sulfate reduction would be suppressed in the most active zones of bioturbation. Additional sulfate reduction and iron reduction rate data are required to prove the dominance of iron reduction in the San Blas sediments, but this relationship between diagenesis and sediment depth may partially explain the excellent shell preservation in the San Blas iron-rich sediments.

## Conclusions

Multiple lines of evidence indicate that, relative to tropical carbonate sediments, skeletal carbonate preservation is enhanced in the mafic-rich siliciclastic sediments that characterize humid tropical arc settings: (1) skeletal carbonate is produced (both by abundant bivalves and by *Halimeda*) and persists in significant amounts in siliciclastic environments; (2) skeletal carbonate is in better condition in siliciclastic sediments than in carbonate sediments, both macroscopically and microscopically, with the exception that in siliciclastics it is prone to secondary precipitates, which enhance preservation; (3) skeletal carbonate persists significantly longer in siliciclastic sediments than in carbonate sediments, based on direct dating of shells; (4) skeletal carbonate is subject to more intense bioerosion in carbonate than in siliciclastic sediments owing to factors linked to grain size, and bioerosion is the primary control on shell destruction; and (5) sediment and pore water geochemistry features indicate that iron-rich siliciclastic sediments favor carbonate preservation over iron-poor carbonate sediments, because as long as sediment reworking does not cause significant degrees of sulfide reoxidation, carbonate dissolution processes are limited in iron-rich sediments.

These findings have several general implications. First, if the best preservation occurs in tropical siliciclastic muds, then bivalve fossil assemblages from siliciclastics should have experienced the least amount of bias due to incomplete preservation. However, due to the greater persistence of shells in such settings, this also implies that time averaging is greater in siliciclastic than in carbonate sediments, assuming comparable sediment accumulation. In contrast, carbonates appear to be settings of much higher rates, if not total magnitude, of shell loss and thus have potential for much more severe taxonomic bias of species richness and differences in proportional abundances. The shorter average persistence of shells, on the other hand, suggests lower degrees of time averaging per assemblage. These taphonomic trade-offs—high capture of diversity but low temporal resolution in siliciclastics versus reduced capture but high temporal resolution in carbonates—suggest quantitative if not qualitative differences in the quality of fossil assemblages from these end-member facies and that the high diversities registered from paleoreef communities are probably minimum estimates (and see Best and Kidwell 2000*a*, 2000*b*; Kidwell et al. 2005).

Second, on a global scale, although it is natural to assume that large river systems such as the Amazon (Aller et al. 1986) probably dominate siliciclastic sediment supply to shallow marine systems, more sediment is probably delivered to coasts via short, steep-gradient rivers in humid tropical areas (Milliman and Syvitski 1992). The mainland coast of San Blas provides a good example of such terrain. Large delta complexes are thus probably not good models for understanding the majority of tropical coastal sedimentation. For example, in contrast to the extensive physical reworking observed at the Amazon and Fly deltas (Alongi 1995; Aller et al. 1996), the coastal bays and inlets of the San Blas coast are protected by offshore carbonate cays and by the various headlands created by river valley flooding during the Holocene sea level rise. In fact, coastlines with small rivers, steep gradients, humid climate weathering, and active tectonics dominated by subduction and mafic lithotypes characterize much of modern-day Central America, northern South America, and Southeast Asia. We expect that our findings in the San Blas Archipelago have relevance for these modern tropical areas, as well as their paleocounterparts.

Finally, tropical siliciclastic shelf facies generated by humid weathering of mafic source areas may be sites of significant carbonate burial due to (1) moderate carbonate production, (2) moderate to high sedimentation, (3) large areal extent of siliciclastics on tropical shelves, (4) lack of exposure of shells at the sediment-water interface (where bioerosion and dissolution are most intense) due to the low grain size of sediment, (5) pore waters that are supersaturated with respect to aragonite during early diagenesis, and (6) "annealing" of shell surfaces by precipitation of authigenic minerals. Budgets for global carbonate burial (e.g., Milliman 1993) tend to ignore the potential of shelf siliciclastics for carbonate burial. However, given the proportion of local carbonate production that may be captured, and the total production in these systems, tropical siliciclastic shelves from humid arc settings may be of the same order of magnitude as

the net accumulation of biogenic carbonate in tropical carbonate shelves.

## ACKNOWLEDGMENTS

We thank the Smithsonian Tropical Research Institute for the use of the San Blas Field Station and for logistical assistance. We also thank dive assistants I. Campbell, O. Barrio, and N. Waltho and lab assistant A. Striegle for their enthusiastic assistance in the field and R. Pillar, E. Bassity, M. Dudley, N. Heim, J. Hansen, M. Handyside, M. Taylor, A. Zimmer, and G. Bowen for their many kinds of lab assistance back in the United States. This project was supported by National Science Foundation–Earth Sciences collaborative grants NSF-EAR 96-28345 to S. M. Kidwell and NSF-EAR 96-28369 to L. M. Walter, and by Smithsonian doctoral fellowships to M. M. R. Best.

## REFERENCES CITED

Alexandersson, E. T. 1979. Marine maceration of skeletal carbonates in the Skagerrak, North Sea. Sedimentology 26:845–852.

Aller, R. C. 1982. Carbonate dissolution in nearshore terriginous muds: the role of physical and biological reworking. J. Geol. 90:79–95.

Aller, R. C.; Blair, N. E.; Xia, Q.; and Rude, P. D. 1996. Remineralization rates, recycling, and storage of carbon in Amazon shelf sediments. Continental Shelf Res. 16:753–786.

Aller, R. C.; Mackin, J. E.; and Cox, R., Jr. 1986. Diagenesis of Fe and S in Amazon inner shelf muds: apparent dominance of Fe reduction and implications for the genesis of ironstones. *In* C. A. Nittrouer and D. J. DeMaster, eds. Sedimentary processes on the Amazon continental shelf. Continental Shelf Res. 6:263–289.

Alongi, D. M. 1992. The influence of freshwater and material export on sedimentary facies and benthic processes within the Fly River Delta and adjacent Gulf of Papua (Papua New Guinea). Continental Shelf Res. 12:287–326.

———. 1995. Decomposition and recycling of organic-matter in muds of the Gulf of Papua, northern coral sea. Continental Shelf Res. 15:1319–1337.

Alongi, D. M.; Tirendi, F.; and Christoffersen, P. 1993. Sedimentary profiles and sediment water solute exchange of iron and manganese in reef-dominated and river-dominated shelf regions of the coral sea. Continental Shelf Res. 13:287–305.

Alongi, D. M.; Tirendi, F.; and Goldrick, A. 1996. Organic carbon oxidation and sediment chemistry in mixed terriginous-carbonate sands of Ningaloo Reef, Western Australia. Mar. Chem. 54:203–219.

Alper, J. 1998. Smithsonian field station gets the boot. Science 280:1340.

Behrensmeyer, A. K.; Kidwell, S. M.; and Gastaldo, R. A. 2000. Taphonomy and paleobiology. Paleobiology 26: 103–147.

Ben-Yaakov, S. 1973. pH buffering of pore water of recent anoxic marine sediment. Limnol. Oceanogr. 18:86–94.

Berner, R. A. 1970. Sedimentary pyrite formation. Am. J. Sci. 268:1–23.

———. 1983. The carbonate-silicate geochemical cycle and its effect on atmospheric carbon dioxide over the past 100 million years. Am. J. Sci. 283:641–683.

Best, M. M. R. 1996. Actualistic bivalve taphonomy in carbonate and siliciclastic tropical marine shelf environments of the San Blas Archipelago, Caribbean Panama. Geol. Soc. Am. annual meeting (Denver), Geol. Soc. Am. Abstr. Program 28:364.

———. 1998. Distribution and nature of siliciclastic and carbonate sediments on the tropical American shelves: significance for carbonate burial. Geol. Assoc. Can. annual meeting (Quebec). Geol. Assoc. Can. Program Abstr. 23:17.

——— 2000. Fates of skeletal carbonate in tropical marine siliciclastic and carbonate sediments, Panama. PhD dissertation, University of Chicago, 309 p.

———. Forthcoming. Contrast in preservation of bivalve death assemblages in siliciclastic and carbonate tropical shelf settings. Palaios.

Best, M. M. R.; Burniaux, P.; and Pandolfi, J. M. 2004. Experimental bivalve taphonomy in reefs of Madang Lagoon, Papua New Guinea. *In* Best, M. M. R., and Caron, J.-B., eds. Canadian Paleontology Conference Proceedings, no. 2. Geol. Assoc. Can. Publ., p. 8–12.

Best, M. M. R., and Kidwell, S. M. 2000*a*. Bivalve taphonomy in tropical mixed siliciclastic-carbonate settings. I. Environmental variation in shell condition. Paleobiology 26:80–102.

———. 2000*b*. Bivalve taphonomy in tropical mixed siliciclastic-carbonate settings. II. Effect of bivalve life habits and shell types. Paleobiology 26:103–115.

Best, M. M. R.; Kidwell, S. M.; Ku, T. C. W.; and Walter, L. M. 1999*a*. Bivalve taphonomy and porewater geochemistry in tropical carbonate and siliciclastic marine environments: implications for the preservation of carbonate. Geol. Assoc. Can. annual meeting (Sudbury). Geol. Assoc. Can. Program Abstr. 24:10.

———. 1999*b*. The role of microbial iron reduction in the preservation of skeletal carbonate: bivalve taphonomy and porewater geochemistry in tropical siliciclastics vs. carbonates. Geol. Soc. Am. Abstr. Program 31:419.

Best, M. M. R.; Ku, T. C. W.; Kidwell, S. M.; and Walter, L. M. 2001. Shells in tropical sediments: skeletons, substrates, and reactive surfaces. Paleobios 21(suppl.): 32.

Brett, C. E., and Baird, G. C. 1986. Comparative taphon-

omy: a key to paleoenvironmental interpretation based on fossil preservation. Palaios 1:207–227.
Broecker, W. S., and Peng, T.-H. 1982. Tracers in the sea. Palisades, NY, Lamont-Doherty Geological Observatory, 690 p.
Canfield, D. E., and Raiswell, R. 1991. Carbonate precipitation and dissolution: its relevance to fossil preservation. *In* Allison, P. A., and Briggs, D. E. G., eds. Taphonomy: releasing the data locked in the fossil record. New York, Plenum, p. 411–453.
Canfield, D. E.; Raiswell, R.; Westrich, J. T.; Reaves, C. M.; and Berner, R. A. 1986. The use of chromium reduction in the analysis of reduced inorganic sulphur in sediments and shales. Chem. Geol. 54:149–155.
Carannante, G.; Esteban, M.; Milliman, J. D.; and Simone, L. 1988. Carbonate lithofacies as paleolatitude indicators: problems and limitations. Sediment. Geol. 60:333–346.
Carroll, M.; Kowalewski, M.; Simoes, M. G.; and Goodfriend, G. A. 2003. Quantitative estimates of time averaging in terebratulid brachiopod shell accumulations from a modern tropical shelf. Paleobiology 29: 381–402.
Case, J. E. 1974. Oceanic crust forms basement of eastern Panama. Geol. Soc. Am. Bull. 85:645–652.
Case, J. E.; Holcombe, T. L.; and Martin, R. G. 1984. Map of the geologic provinces in the Caribbean region. *In* Bonini, W. E.; Hargraves, R. B.; and Shagam, R., eds. The Caribbean–South America plate boundary and regional tectonics. Boulder, CO, Geol. Soc. Am. Mem. 162:1–30.
Clifton, K. E. 1997. Mass spawning by green algae on coral reefs. Science 275:1116–1118.
Clifton, K. E.; Kim, K.; and Wulff, J. L. 1997. Field guide to the reefs of Caribbean Panamá with an emphasis on western San Blas. Proceedings of the 8th International Coral Reef Symposium (Panama City, Panama). 1:167–184.
Coates, A. G., and Obando, J. A. 1996. The geologic evolution of the Central American Isthmus. *In* Jackson, J. B. C.; Budd, A. F.; and Coates, A. G., eds. Evolution and environment in tropical America. Chicago, University of Chicago Press, p. 21–56.
Cubit, J. D.; Caffey, H. M.; Thompson, R. C.; and Windsor, D. M. 1989. Meteorology and hydrography of a shoaling reef flat on the Caribbean coast of Panama. Coral Reefs 8:59–66.
D'Croz, L., and Robertson, D. R. 1997. Coastal oceanographic conditions affecting coral reefs on both sides of the Isthmus of Panama. Proceedings of the 8th International Coral Reef Symposium (Panama City, Panama). 2:2053–2058.
D'Croz, L.; Robertson, D. R.; and Martinez, J. A. 1999. Cross-shelf distribution of nutrients, plankton, and fish larvae in the San Blas Archipelago, Caribbean Panama. Rev. Biol. Trop. 47:203–215.
Doyle, L. J., and Roberts, H. H., eds. 1988. Carbonate-clastic transitions. Developments in sedimentology. Vol. 42. Amsterdam, Elsevier.
Escalante 1990. The geology of southern Central America and western Colombia. *In* Dengo, G., and Case, J. E. eds. The Caribbean region (Geology of North America, Vol. H). Boulder, CO, Geol. Soc. Am., p. 201–230.
Fornos, J. J.; Forteza, V.; Jaume, C.; and Martinez-Taberner, A. 1992. Present-day Halimeda carbonate sediments in temperate Mediterranean embayments: Fornells, Balearic Islands. Sediment. Geol. 75:283–293.
Freile, D., and Hillis, L. 1997. Carbonate productivity by *Halimeda incrassata* in a land proximal lagoon, Pico Feo, San Blas, Panama. Proceedings of the 8th International Coral Reef Symposium (Panama City, Panama). 1:767–772.
Freile, D.; Milliman, J. D.; and Hillis, L. 1995. Bank-edge *Halimeda* meadow, western Great Bahama Bank, and its sedimentary importance. Coral Reefs 14:27–33.
Furukawa, Y.; Bentley, S. J.; Shiller, A. M.; Lavoie, D. L.; and Van Cappellen, P. 2000. The role of biologically-enhanced pore water transport in early diagenesis: an example from carbonate sediments in the vicinity of North Key Harbor, Dry Tortugas National Park, Florida. J. Mar. Res. 58:493–522.
Gieskes, J. M., and Rogers, W. C. 1973. Alkalinity determinations in interstitial waters of marine sediments. J. Sediment. Petrol. 43:272–277.
Glover, C. P., and Kidwell, S. M. 1993. Influence of organic matrix on the postmortem destruction of molluscan shells. J. Geol. 101:729–747.
Granier, B.; Villain, J. M., and Boichard, R. 1996. Biohermes holocènes à Halimeda au large du delta de la Mahakam, Kalimantan, Indonésie: le concept de "section condensée dilatée": carbonates intertropicaux. Mém. Soc. Géol. Fr. 20:225–230.
Green, M. A., and Aller, R. C. 1998. Seasonal patterns of carbonate diagenesis in nearshore terrigenous muds: relation to spring phytoplankton bloom and temperature. J. Mar. Res. 56:1097–1123.
———. 2001. Early diagenesis of calcium carbonate in Long Island Sound sediments: benthic fluxes of $Ca^{2+}$ and minor elements during seasonal periods of net dissolution. J. Mar. Res. 59:769–794.
Green, M. A.; Aller, R. C.; and Aller, J. Y. 1993. Carbonate dissolution and temporal abundances of Foraminifera in Long Island Sound sediments. Limnol. Oceanogr. 38:331–345.
Hammer, Ø.; Harper, D. A. T.; and Ryan, P. D. 2001. PAST: palaeontological statistics software package for education and data analysis. Palaeontol. Electronica 4:9.
Harper, E. M. 2000. Are calcitic layers an effective adaptation against shell dissolution in the Bivalvia? J. Zool. 251:179–186.
Hutchings, P. A. 1986. Biological destruction of coral reefs. Coral Reefs 4:239–252.
James, N. P. 1997. The cool-water carbonate depositional realm. *In* James, N. P., and Clarke, J. A. D., eds. Cool-water carbonates. SEPM Spec. Publ. 56:1–20.
James, N. P.; Bone, Y.; and Kyser, T. K. 2005. Where has all the aragonite gone? mineralogy of holocene neritic cool-water carbonates, southern Australia. J. Sediment. Res. 75:454–463.

Jorgensen, B. B. 1982. Mineralization of organic-matter in the sea bed: the role of sulfate reduction. Nature 296:643–645.

Kaufman, D. S., and Manley, W. F. 1998. A new procedure for determining enantiomeric (D/L) amino acid ratios in fossils using reverse phase liquid chromatography. Quat. Sci. Rev. 17:987–1000.

Kesler, S. E.; Levy, E.; and Martin, F. C. 1990. Metallogenic evolution of the Caribbean region. *In* Dengo, G., and Case, J. E, eds. The Caribbean region (Geology of North America, Vol. H). Boulder, CO, Geol. Soc. Am., p. 459–482.

Kesler, S. E.; Sutter, J. F.; Issigonis, M. J.; Jones, L. M.; and Walker, R. L. 1977. Evolution of porphyry copper mineralization in an oceanic island arc: Panama. Econ. Geol. 72:1142–1153.

Kidwell, S. M.; Best, M. M. R.; and Kaufman, D. S. 2005. Taphonomic tradeoffs in tropical marine death assemblages: differential time-averaging, shell loss, and probable bias in siliciclastic versus carbonate facies. Geology 33:729–732.

Kidwell, S. M.; Rothfus, T.; and Best, M. M. R. 2001. Sensitivity of taphonomic signatures to sample size, sieve size, damage scoring system, and target taxa. Palaios 16:26–52.

Kostka, J. E.; Haefele, E.; Viehweger, R.; and Stucki, J. W. 1999. Respiration and dissolution of iron(III) containing clay minerals by bacteria. Environ. Sci. Technol. 33:3127–3133.

Kostka, J. E.; Stucki, J. W.; Nealson, K. H.; and Wu, J. 1996. Reduction of structural Fe(III) in smectite by a pure culture of *Shewanella putrefaciens* strain MR-1. Clays Clay Min. 44:522–529.

Ku, T. C. W. 2001. Organic carbon-minerals interactions in terrestrial and shallow marine environments. PhD dissertation, University of Michigan, Ann Arbor, 318 p.

Ku, T. C. W., and Walter, L. M. 2003. Syndepositional formation of Fe-rich clays in tropical shelf sediments, San Blas Archipelago, Panama. Chem. Geol. 197:197–213.

Ku, T. C. W.; Walter, L. M.; Best, M. M. R.; and Kidwell, S. M. 2000. The role of reactive iron aluminosilicates in carbonate preservation during early marine diagenesis of coastal sediments, San Blas Archipelago, Panama. Geol. Soc. Am. annual meeting (Reno, NV). Geol. Soc. Am. Abstr. Program 32:A-77.

Ku, T. C. W.; Walter, L. M.; Coleman, M. L.; Blake, R. E.; and Martini, A. M. 1999. Coupling between sulfur recycling and syndepositional carbonate dissolution: evidence from oxygen and sulfur isotope composition of pore water sulfate, South Florida Platform, USA. Geochim. Cosmochim. Acta 63:2529–2546.

Kukal, Z. 1990. The rate of geological processes. Earth Sci. Rev. 28:94–135.

Lees, A. 1975. Possible influence of salinity and temperature on modern shelf carbonate sedimentation. Mar. Geol. 19:159–198.

Leinfelder, R. 1997. Coral reefs and carbonate platforms within a siliciclastic setting: general aspects and examples from the Late Jurassic of Portugal. Proceedings of the 8th International Coral Reef Symposium (Panama City, Panama) 2:1737–1742.

MacIntyre, I. G.; Glynn, P. W.; and Steneck, R. S. 2001. A classic Caribbean algal ridge, Holandes Cays, Panama: an algal-coated storm deposit. Coral Reefs 20: 95–105.

Manly, B. F. J. 1994. Multivariate statistical methods: a primer. London, Chapman & Hall, 214 p.

Mann, P., and Kolarsky, R. A. 1995. East Panama deformed belt: structure, age, and neotectonic significance. Geol. Soc. Am. Spec. Pap. 295:111–130.

Maury, R. C.; Defant, M. J.; Bellon, H.; de Boer, J. Z.; Stewart, R. H.; and Cotten, J. 1995. Early Tertiary arc volcanics from eastern Panama. Geol. Soc. Am. Spec. Pap. 295:29–34.

Mehrbach, C.; Culberso, C.; Hawley, J. E.; and Pytkowic, R. 1973. Measurement of apparent dissociation constants of carbonic acid in seawater at atmospheric pressure. Limnol. Oceanogr. 18:897–907.

Millero, F. J. 1979. The thermodynamics of the carbonate system in seawater. Geochim. Cosmochim. Acta 43: 1651–1661.

———. 1995. Thermodynamics of the carbon dioxide system in the oceans. Geochim. Cosmochim. Acta 59: 661–677.

Milliman, J. D. 1993. Production and accumulation of calcium carbonate in the ocean: budget of a nonsteady state. Global Biogeochem. Cycles 7:927–957.

Milliman, J. D., and Droxler, A. W. 1995. Calcium carbonate sedimentation in the global ocean: linkages between the neritic and pelagic environments. Oceanography 8:92–94.

Milliman, J. D., and Syvitski, J. P. M. 1992. Geomorphic/tectonic control of sediment discharge to the ocean: the importance of small mountainous rivers. J. Geol. 100:525–544.

Morse, J. W.; Zullig, J. J.; Bernstein, L. D.; Millero, F. J.; Milne, P.; Mucci, A.; and Choppin, G. R. 1985. Chemistry of calcium carbonate rich shallow-water sediments in the Bahamas. Am. J. Sci. 285:147–185.

Mount, J. F. 1984. Mixing of siliciclastic and carbonate sediments in shallow shelf environments. Geology 12: 432–435.

Mucci, A. 1983. The solubility of calcite and aragonite in seawater at various salinities, temperatures, and one atmosphere total pressure. Am. J. Sci. 283:780–799.

Odin, G. S. 1990. Clay mineral formation at the continent-ocean boundary: the verdine facies. Clay Miner. 25:477–483.

Opdyke, B. N., and Walker, J. C. G. 1992. Return of the coral reef hypothesis: basin to shelf partitioning of $CaCO_3$ and its effect on atmospheric $CO_2$. Geology 20:733–736.

Peakall, R., and Smouse, P. E. 2006. GENALEX 6: genetic analysis in Excel. Population genetic software for teaching and research. Mol. Ecol. Notes 6:288–295.

Raiswell, R., and Canfield, D. E. 1996. Rates of reaction between silicate iron and dissolved sulfide in Peru

Margin sediments. Geochim. Cosmochim. Acta 60: 2777–2787.
———. 1998. Sources of iron for pyrite formation in marine sediments. Am. J. Sci. 298:219–245.
Raiswell, R.; Canfield, D. E.; and Berner, R. A. 1994. A comparison of iron extraction methods for the determination of degree of pyritisation and the recognition of iron-limited pyrite formation. Chem. Geol. 111: 101–110.
Roberts, H. H. 1987. Modern carbonate-siliciclastic transitions: humid and arid tropical examples. Sediment. Geol. 50:25–65.
Roberts, H. H., and Sydow, J. 1997. Siliciclastic-carbonate interactions in a tropical deltaic setting: Markham delta of east Kalimantan, Indonesia. Proceedings of the 8th International Coral Reef Symposium (Panama City, Panama) 2:1773–1778.
Sadler, J. C.; Lander, M. A.; Hori, A. M.; and Oda, L. K. 1987. Tropical marine climatic atlas. Vol. I. Indian Ocean and Atlantic Ocean. Honolulu, University of Hawaii.
Sare, V. P., and Humphrey, J. D. 1997. Carbonate ramp sands of the San Blas Islands, Panama, and the effects of meteoric diagenesis. American Association of Petroleum Geologists annual convention (Tulsa, OK). Am. Assoc. Pet. Geol. and Soc. Econ. Paleontol. Mineral. 6:101–102.
Shulman, M. J., and Robertson, D. R. 1996. Changes in the coral reefs of San Blas, Caribbean Panama: 1983 to 1990. Coral Reefs 15:231–236.
Sokal, R. R., and Rohlf, F. J. 1995. Biometry. New York, W. H. Freeman, 887 p.
Taylor, J. D.; Kennedy, W. J.; and Hall, A. 1969. The shell structure and mineralogy of the Bivalvia. Introduction. Nuculacea-Trigonacea. Bull. Br. Mus. (Nat. Hist.) Zool. Suppl. 3:1–125.
———. 1973. The shell structure and mineralogy of the Bivalvia. II. Lucinacea-Clavagellacea. Conclusions. Bull. Br. Mus. (Nat. Hist.) Zool. 22:253–294.
U.S. Department of Defense. 1984. Approach to Golfo de San Blas. Defense Mapping Agency chart 26065.
Verardo, D.; Froelich, P.; and McIntyre, A. 1990. Determination of organic carbon and nitrogen in marine sediments using the Carlo-Erba NA-1500 analyzer. Deep-Sea Res. 37:157–165.
Walter, L. M., and Burton, E. A. 1990. Dissolution of recent platform carbonate sediments in marine pore fluids. Am. J. Sci. 290:601–643.
Woodring, W. P. 1957. Geology and paleontology of Canal Zone and adjoining parts of Panama: geology and description of Tertiary mollusks (Gastropods: Trochidae to Turritellidae) U.S. Geol. Surv. Prof. Pap. 306-A, p. 1–145, plates 1–23 (including two maps).